Characterization of phase changes during fabrication of copper alloys, crystalline and non-crystalline, prepared by mechanical alloying

Caracterización de los cambios de fases en la fabricación de aleaciones base cobre, cristalinas y no cristalinas, por aleado mecánico

P.A. Rojas[1], C. Martínez[2], C. Aguilar[3], F. Briones[4], M. E. Zelaya[5], and D. Guzmán[6]

ABSTRACT

The manufacture of alloys in solid state has many differences with the conventional melting (casting) process. In the case of high energy milling or mechanical alloying, phase transformations of the raw materials are promoted by a large amount of energy that is introduced by impact with the grinding medium; there is no melting, but the microstructural changes go from microstructural refinement to amorphization in solid state. This work studies the behavior of pure metals (Cu and Ni), and different binary alloys (Cu-Ni and Cu-Zr), under the same milling/mechanical alloying conditions. After high-energy milling, X ray diffraction (XRD) patterns were analyzed to determine changes in the lattice parameter and find both microstrain and crystallite sizes, which were first calculated using the Williamson-Hall (W-H) method and then compared with the transmission electron microscope (TEM) images. Calculations showed a relatively appropriate approach to observations with TEM; however, in general, TEM observations detect heterogeneities, which are not considered for the W-H method. As for results, in the set of pure metals, we show that pure nickel undergoes more microstrain deformations, and is more abrasive than copper (and copper alloys). In binary systems, there was a complete solid solution in the Cu-Ni system and a glass-forming ability for the Cu-Zr, as a function of the Zr content. Mathematical methods cannot be applied when the systems have amorphization because there are no equations representing this process during milling. A general conclusion suggests that, under the same milling conditions, results are very different due to the significant impact of the composition: nickel easily forms a solid solution, while with a higher zirconium content there is a higher degree of glass-forming ability.

Keywords: Copper based alloys, mechanical alloying, X ray diffraction, transmission electron microscopy.

RESUMEN

La fabricación de aleaciones en estado sólido tiene muchas diferencias con el proceso de fusión (colada) convencional. En el caso de la molienda de alta energía o aleado mecánico, las trasformaciones de fases de las materias primas son promovidas por una gran cantidad de energía que se introduce mediante impacto con medios de molienda; no hay fusión, pero sí cambios microestructurales que van desde refinamiento microestructural hasta amorfización en estado sólido. En este trabajo se estudia el comportamiento de metales puros (Cu y Ni) y diferentes aleaciones binarias (Cu-Ni y Cu-Zr) sometidas a las mismas condiciones de molienda con el objetivo de analizar el efecto del proceso en metales similares (Cu y Ni) y con solubilidades muy diferentes (Cu-Ni y Cu-Zr). Después de la molienda de alta energía, se analizaron los patrones de difracción de rayos X para determinar cambios en parámetros de red, y calcular las micro-deformaciones y el tamaño de las cristalitas, los cuales fueron calculados por el método de Williamson Hall (W-H), para luego ser comparados con los datos de las imágenes obtenidas por microscopía electrónica de transmisión (MET). Los cálculos muestran una apropiada similitud con las observaciones en MET; sin embargo, en general, las observaciones muestran heterogeneidades que no son consideradas en el método de W-H. De acuerdo a los resultados, en los metales puros se observó mayor cantidad de micro-deformaciones en níquel y fue más abrasivo que el cobre. En las aleaciones binarias, el sistema Cu-Ni formó soluciones sólidas con solubilidad total y las del sistema Cu-Zr mostraron amorfización, en función del contenido de Zr. Los métodos matemáticos no pueden ser aplicados en los casos donde se detecta amorfización debido a que aún no han sido creadas ecuaciones que representen este fenómeno cuando ocurre durante la molienda. Como conclusión se observó que bajo las mismas condiciones de molienda los resultados pueden ser muy diferentes debido al impacto significativo de la composición: el níquel formó fácilmente solución sólida mientras que el circonio incremento la habilidad de formación de vidrios.

Palabras clave: Aleaciones base cobre, aleado mecánico, difracción de rayos X, microscopía electrónica de transmisión.

Introduction

The possibility of manufacturing new materials with new properties has been one of the most important goals in mechanical alloying processes. More than fifty years after its development, and beyond simple milling parameters, many systems have demonstrated extraordinary abilities, never obtained with other manufacturing methods; one such example is glass forming in binary systems (Benjamin, 1970; Benjamin, 1974; Schwarz, 1986; Davis, 1988; Calka, 1991; Maurice, 1994; Lü, 1998). In this same line, mechanically alloyed and milled powder both have been shown to display a variety of microstructural changes; indeed, using this process, it has been possible to produce a variety of nonequilibrium phases such as supersaturated solid solutions, metastable intermediate phases, quasicrystalline alloys, nanostructured materials and metallic glasses (Suryanarayana, 1995; Suryanarayana 2004; Suryanarayana 2011). However, many of these qualities overlap during mechanical processes, making it more difficult to understand the nature of changes. For this reason, in this paper pure metals and binary copper-based alloys are studied under the same milling conditions in order to attempt to separate the effects of the experimental parameters on the resulting composition of effects, which include the microstrain, crystallite size, and glass forming ability.

Experimental procedures

The mechanical milling and mechanical alloying were performed with pure powders: Cu (>99,7% pure, fine powder particle size <63 μm, >230 mesh ASTM, Merck), Ni (>99% pure, <230 mesh ASTM, Merck), and Zr (>99,8% pure. <50 mesh ASTM, Noah Tech). The high-energy milling was performed in a SPEX 8000D mill using stainless steel containers and balls. The ball to powder ratio (BPR) in all cases was 10:1. The containers were filled in a glove box with an argon atmosphere, and included 1 weight percent (wt%) of stearic acid as the control agent. The modified variable was the milling time, which was varied from 1 to 60 hours. After milling, the powders were removed from the containers inside an Ar-filled glove box. The milled samples were analyzed by X-ray diffraction (XRD) in a Shimadzu XDR-6000 diffractometer using Cu Kα radiation. The iron content was measured using a GBS 905 atomic absorption

[1] PhD. In Engineering. Affiliation: Universidad Adolfo Ibáñez, Chile.
E-mail: paula.rojas.s@uai.cl.

[2] PhD. in Engineering. Affiliation: Universidad Adolfo Ibáñez, Chile.
E-mail: carola.martinez@pd.uai.cl

[3] PhD. in Engineering. Affiliation: Universidad Tecnológica Federico Santa María, Chile. E-mail: claudio.aguilar@usm.cl.

[4] MSc. in Metallurgy. Affiliatison: Universidad Tecnológica Federico Santa María, Chile.

[5] PhD. in Physics. Affiliation: Centro Atómico Bariloche. Argentina.
E-mail: euge.zelaya@gmail.com

[6] PhD. in Engineering. Affiliation: Universidad de Atacama, Chile.
E-mail: danny.guzman@uda.cl

spectrometer, while the microstructural observations were carried out in a Philips CM200UT microscope. A step by step deposition of particles on TEM grid is described as follows: 1) The sample is settled in an alcohol solution (ethanol). 2) The sample is homogenized in alcohol. 3) The alcohol suspension is dropped over the Lacey Carbon - copper TEM grid. The alcohol is evaporated and the samples are retained in the grid. The sample is set in the sample holder of the TEM.

Results and discussion

Copper and Nickel high-energy milling

The XRD spectra corresponding to the different samples, milled from 1 to 60h, using pure Cu and Ni powders, are shown in Figure 1. X-ray diffraction peak analysis was performed through application of the Williamson–Hall method. According to the calculated crystallite size (Figure 2), copper quickly reaches a value below 20 nanometers, which is a value in the range reported by other authors (Suryanarayana, 2001; Fecht, 1990; Delogu, 2006), and is associated with strong microstructural refinement during the process; however, nickel in this process behaved differently, instead of reaching values of 10 nm after 60 hours of milling, which is relatively low for FCC metals. As shown in the results, the same milling conditions differently affect these two metals. For nickel, the milling process was not just a structural refinement process; rather, the displacement of the diffraction peaks shows another phenomenon not observed in copper and not associated with the sources of strain, which often affect diffractograms (peak shift, peak broadening, asymmetry, or shape) (Ungar, 2004). To analyze these differences, the Williamson-Hall method was used to quantify the structural refinement during mechanical milling (crystallite sizes and microstrain). This method has been frequently used in this type of materials because it is a good approximation for values measured with a TEM microscope (or others, calculated with more complex methods) (Nazari, 2013; Kursun, 2015). Williamson and Hall demonstrated that the integral width (IW) of a 2h diffraction peak can be decomposed into a contribution due to a finite scattering volume and a contribution due to local fluctuations in strain. The IW is formally defined as the integral of the peak profile divided by the peak height (Brandstetter, 2008). Calculations show that the microstrain was higher in nickel, thus generating a harder and more abrasive material (Figure 2). Additionally, the composition of the powder after milling was analyzed by atomic absorption spectroscopy (AAS). The results of this spectroscopy showed a high Fe% content in the nickel powders. Iron is a contaminant that has been observed in some cases, because the milling media (balls) and the container are made of steel, (Suryanarayana, 1995; Suryanarayana 2004; Suryanarayana 2011) but in general, the contamination is smaller (<1%) than this study. The results of the analyzes show that with 60 hours of milling, the nickel samples had around 14% wt. of Fe, while, copper with the same time had less than 1% wt. Despite these results, XRD analyzes did not show iron peaks. The

diffraction patterns show a displacement of the nickel peaks; this displacement of the diffraction peaks and the increase in the lattice parameter determined in the Ni might be explained if portions of the iron were dissolved into the nickel structure; however, since the atomic radius of iron is lower than nickel, then the expected effect of solid solution formation would be a smaller lattice parameter. These effects could be related to the fact that the solid solution is not being made in the traditional way, a high microstrain (Figure 2) accompanies the introduction of the iron atoms in the nickel network, which could produce these alterations in the lattice parameter. It is necessary to remember that these conditions are very far from the thermodynamic equilibrium. In fact, according to the phase equilibrium diagrams, copper and nickel have a very different relationship with iron. While iron has a very low solubility in copper, which reaches 4,1 wt. % at 1096 °C; iron in nickel can have a 100% solubility, when it is face centered cubic structure (FCC). Also, nickel and iron react, forming intermetallic compounds (Fe_3Ni, $FeNi$, $FeNi_3$) none of which was detected by XRD.

Furthermore, nano-indentation hardness and elastic modulus of the sample of Ni with 5h of milling was determined. Sampling consisted of 60 points, determining the average hardness value 9,31 GPa with a standard deviation s=0,99 and a value corresponding to 167,80 GPa elastic modulus with a standard deviation s=16,77. These values show that, after 5 hours of milling, the elastic modulus remained. However, the hardness was increased more than 5 times compared to normal values.

Copper and nickel milling, mechanical alloying

Supersaturated solid solutions produced by mechanical alloying have been studied (Rojas, 2006; Betancourt, 2012; Bera, 2012; Hamzaoui, 2014; Kubaloba, 2014; Contini, 2014; Loureiro, 2014; Barzegar, 2014; Aguilar, 2014; Kumar, 2015; Wu, 2015; Qiang, 2015; Loginov, 2015). That said, Cu and Ni have extended solid solutions; as such, part of this study had the goal of determining how much milling time was required to make the solid solution and of defining which one acts as solvent.
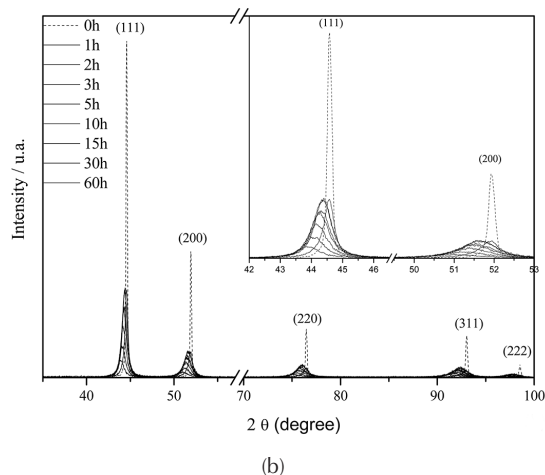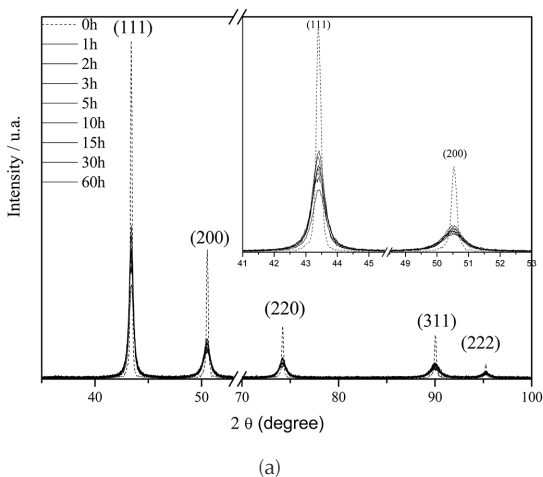

(a)

(b)

Figure 1. XRD spectra of pure Cu and Ni after different milling times, under the same milling conditions: a) pure Cu (o) and b) pure Ni (+).
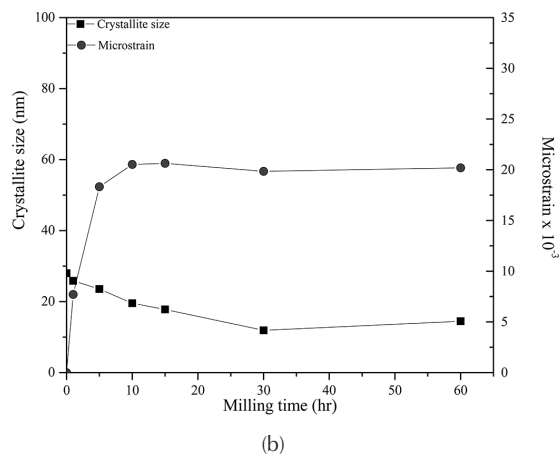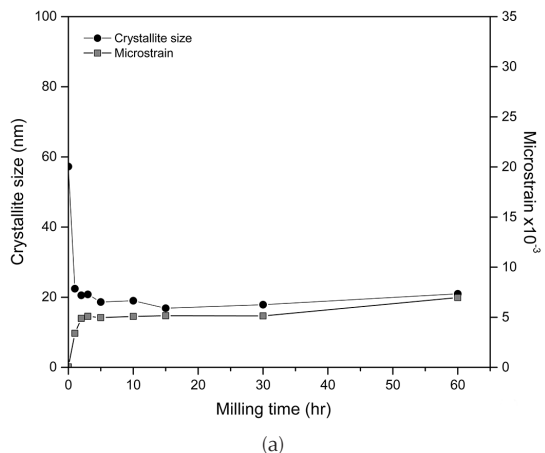

(a)

(b)

Figure 2. Calculated crystallite size and microstrain as a function of milling time of: a) pure Cu and b) pure Ni.

The diffraction patterns show that, with 5 hours of milling, the solid solution is obtained (Figure 3). With increased milling time, the intensity of Ni peaks decreases, and the Ni content of the powders was gradually dissolved into the Cu phase. According to these results, alloying mechanically Cu and Ni, copper was the solvent and

nickel was the solute. The Williamson-Hall method was used to obtain the crystallite size and microstrain in these alloys (Figure 4). The crystallite size here was larger than that of either of the pure metals and almost constant after 30 hours of milling. The microstrain was greater in both alloys, with respect to pure copper (Figure 2a), although more similar to pure nickel; we recall that this latter was contaminated with iron, suggesting that it was a solid solution. In the Cu-Ni alloys, this increase in microstrain may be related not only to solid solution strengthening and iron (as was the case with nickel), but also with nickel dissolving into the copper. Tellingly, the results of chemical analysis show iron contamination at an intermediate level compared to the pure, milled elements; this demonstrates a correlation between iron content in the powders after milling and the percentage of nickel of the sample before milling. In short, samples containing some percentage of nickel always ended their millings with a higher content of iron contamination.
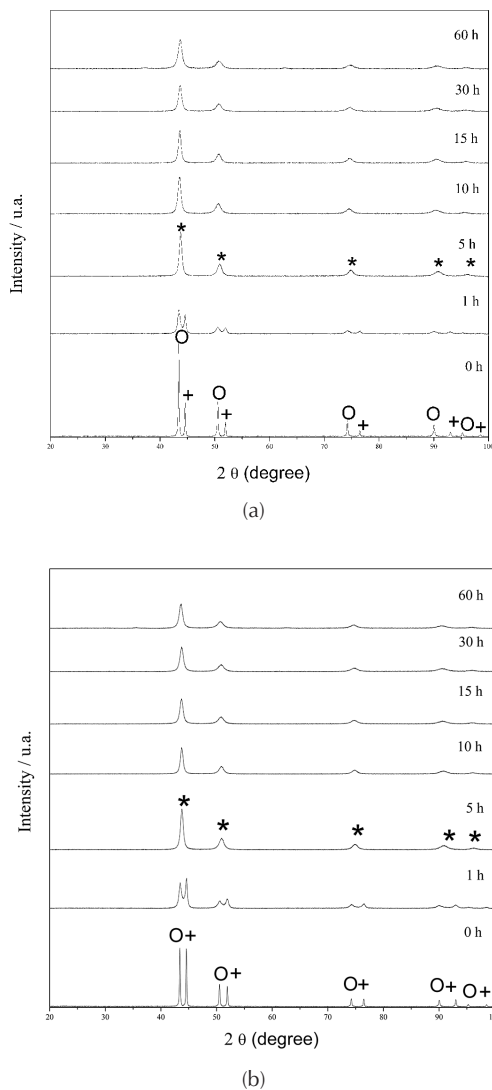

(a)

(b)

Figure 4. Calculated crystallite size and microstrain as a function of milling time of: a) 60%Cu- 40% Ni -and b) 50%Cu- 50% Ni.

Copper and zirconium milling, mechanical alloying

Copper and zirconium do not have as high a solid solubility as do Cu and Ni; rather, these elements form many intermediate phases, as shown in their binary phase diagrams (Arias, 1990; He, 2006; Okamoto, 2008). For over 20 years, it has been known that Cu and Zr together have an excellent glass forming ability, proven by different methods of fabrication (Chen, 1993; Brunelli, 2001; Xu, 2004; Zhang, 2009; Du, 2014; Ristic, 2015). In order to compare the changes in the phases in the Cu-Ni and Cu-Zr systems in this study, the same mechanical alloying conditions were used for both systems. As shown in the results (Figure 3 and Figure 5), for the two binary systems in study, Cu-Ni and Cu-Zr, the structural changes are totally different, even under exactly the same milling conditions: in one system Cu-Ni, the nickel is dissolved into copper; in the other Cu-Zr, the zirconium is not dissolved, but rather promotes the loss of crystallinity in copper. In both cases, after 5 hours of milling, the peak intensity decreases, and just two broad peaks are observed. In Cu-Zr case, it was not possible to apply the Williamson-Hall method. For that reason, to compare Cu-Zr alloys milled with pure milled Cu and pure milled Ni, the study made use of TEM microscopy.

(a)

(b)

Figure 3. XRD spectra of pure Cu-Ni alloys after different milling times, under the same milling conditions (o Cu; + Ni): a) 60%Cu- 40% Ni -and b) 50%Cu- 50% Ni. (o Cu; + Ni, * ss).
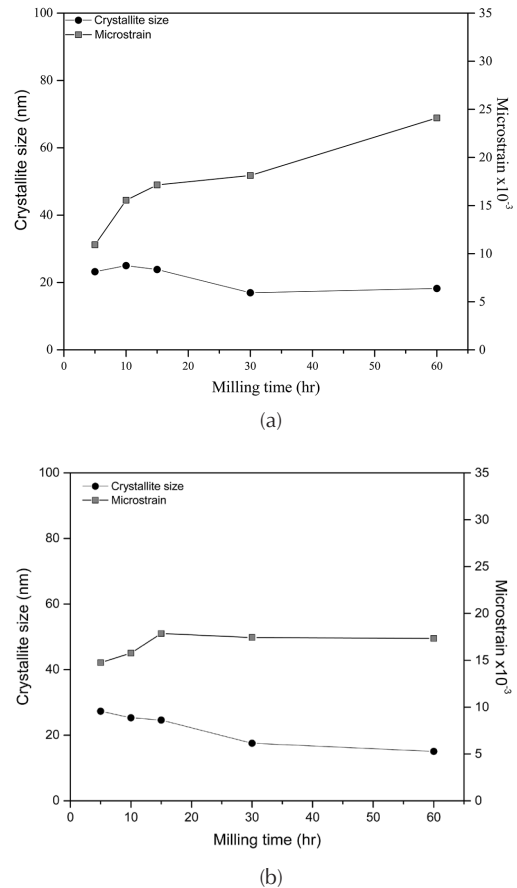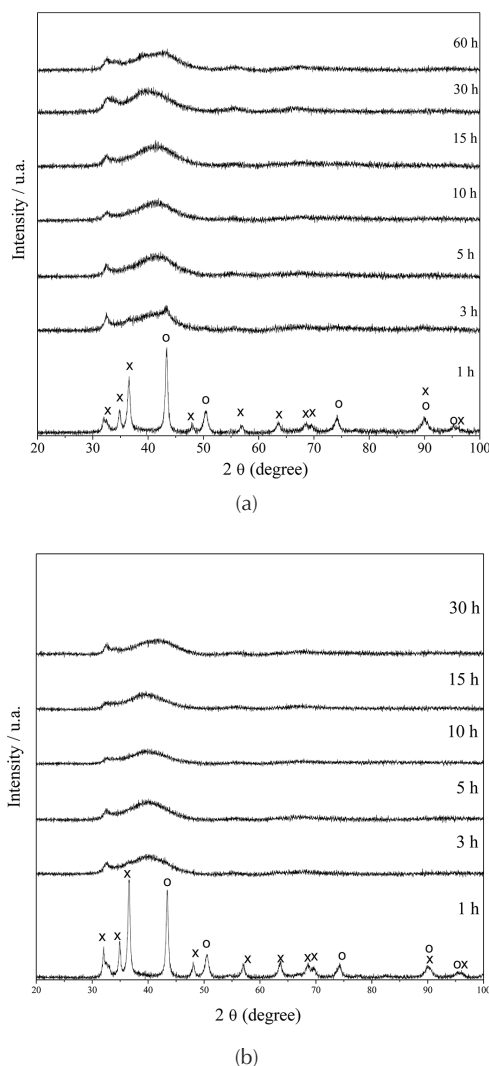
(a)

(b)

(a)

(b)

(c)

(d)

Figure 6. Images of bright field and dark field pure copper particles: a) 5 h bright field, b) 5 h dark field, c) clear field and d) dark field with 60 h.

(a)

(b)

(c)

(d)

Figure 7. Images of bright field and dark field pure nickel particles a) bright field Ni 5 h, b) dark field Ni 5h, c) bright field - Fe 2,3 % and Ni 97,7 % (60h), d) dark field Fe 2,3 % and Ni 97,7 % (60 h).

In Figure 7d, another image is shown with the typical doubled contrast for those areas with high deformation. The dashed arrow points to a typical grain size, while whole white arrows indicate an area of high deformation. The data observed in the transmission electron microscopy agree with those calculated by the Williamson-Hall method (Figure 2b). TEM analysis was performed on the Cu – Zr (60-40) alloy, after 5 hours of milling. By examining this sample, three types of particles were observed, and appear

(a)

(b)

Figure 5. XRD spectra of pure Cu-Zr alloys after different milling times, under the same milling conditions: a) 60 %Cu- 40 % Zr -and b) 50 %Cu- 50 % Zr.

Figure 6 shows the bright field (Figure 6a and Figure 6c) and dark field (Figure 6b and Figure 6d) of the same particle of pure copper. There is a wide range of mean particle diameter, between 15 nm and 150 nm for Cu 5 h (Figure 6a and Figure 6b), and from 5 to 35 nm for Cu 60 h (Figure 6c and 6d). The data observed in the transmission electron microscopy agree with those calculated by the Williamson-Hall method (Figure 2a). In Figure 7a, a detail of the microstructure of a Ni particle is observed after 5 hours of milling, and has a mean diameter of 2 mm; as can be seen, the grain boundaries are rather diffuse. In Figure 7b, the detail of a dark field performed on an area of Ni particle after 5 h is shown. While grain boundaries remain somewhat diffuse, a wide range average grain diameter is revealed to be between 15 and 200 nm. In the case of the dark field image of the Ni sample after 60 h of milling, there are areas where you can find a few grains of average diameter ~ 120 nm. However, such grains show high deformation.
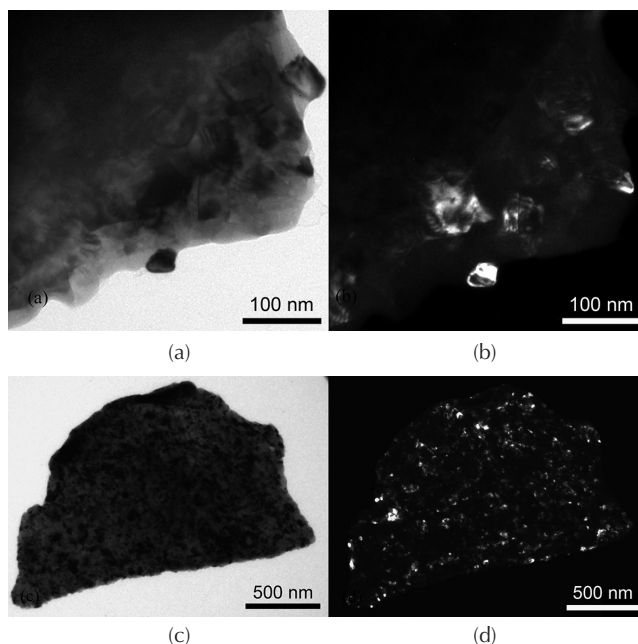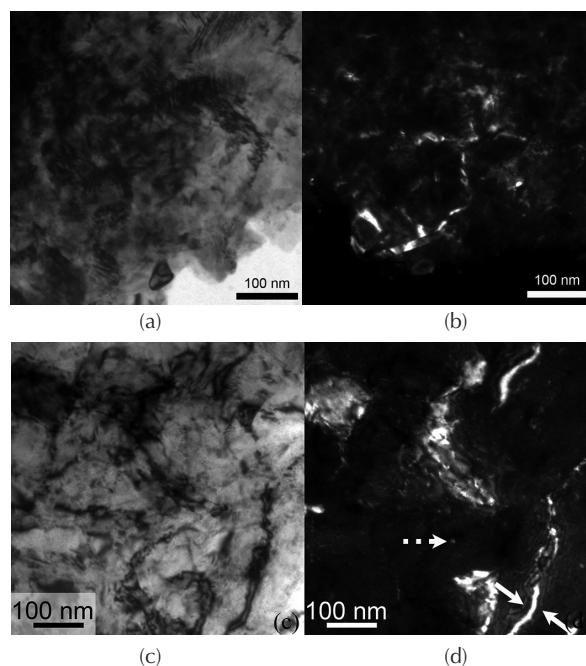
to reveal three different states: the first stage, in which the particles begin to integrate Cu into Zr while retaining the microstructural characteristics of Cu (type 1 particles, Figure 8a and Figure 8b), and in which Zr also appears as disintegrated particles; the second state, where the grain size is of an order of magnitude smaller due to grain refinement produced by the inclusion of Zr, (Figures 8c and Figure 8d), and in which it appears that Zr milling induces a strong amount of dislocation, which aids in further refining the grain size; and the third and final state, where the inclusion of Zr in the Cu produces an amorphous structure, due to reduced grain size inducing dislocations (Figure 8e), and for which this type of particle has an atomic percentage of Zr of around 25 %. The diffraction patterns of these particles correspond to highly amorphous materials. Figure 10 clearly shows both amorphous halos belonging to the material, as well as some small diffractions stemming from the remaining crystalline material (white arrow).
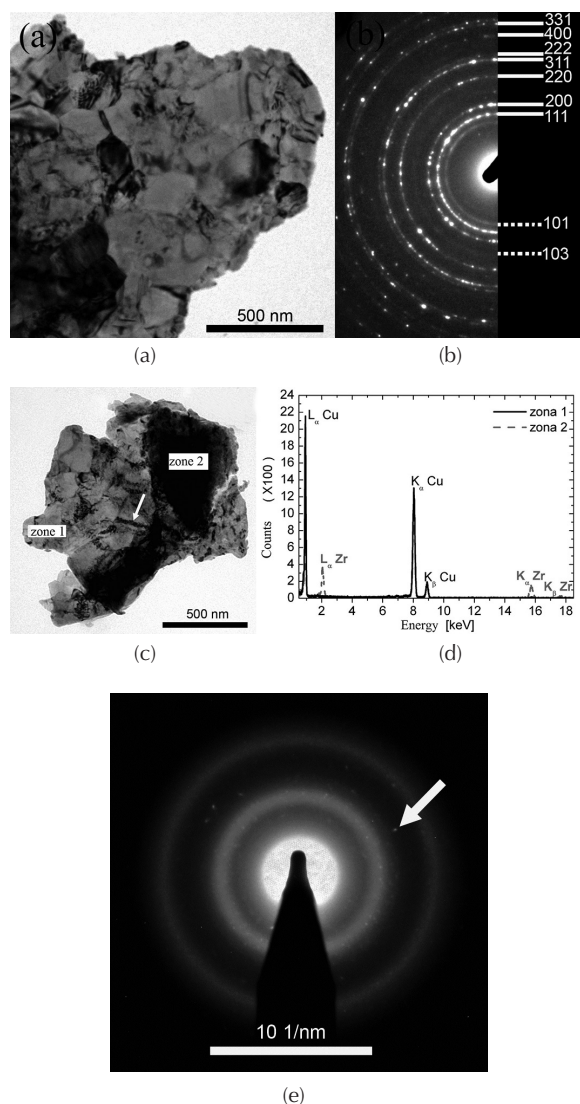

Figure 8. Particle type 1: a) Bright field micrograph and b) diffraction pattern of Cu - Zr particle. Particle type 2: c) bright field image, d) energy spectrum of two zones of Cu- Zr particles. Particle type 3: e) Diffraction pattern of a Cu - Zr particle with about 25 % Zr.

Conclusions

When pure nickel and pure copper are separately subjected to high-energy milling under the same conditions, even though they reach similar crystallite size, the microstrain is much higher in nickel, which produces a high degree of hardening in that metal. The high degree of hardening in nickel, in turn, promotes abrasion of the container and balls, generating a high content of iron in powders and solutions.

The crystalline phase changes during fabrication of copper-based alloys prepared by mechanical alloying is not homogeneous as demonstrated with the results of transmission electron microscopy compared with those calculated from the diffraction profiles.

For mechanical alloying of Cu and Ni, under the same conditions and after five hours, a complete solid solution was achieved. Mechanical alloying of Cu and Zr, under the same conditions and after five hours, shows there is a substantial loss of crystallinity, especially in the areas richest in zirconium.

Williamson–Hall method is a good approximation in mechanically milled pure metals because it shows differences in the phases, but when milling involves more elements, which form solid solutions or amorphous phases, transmission electron microscopy is more useful to understand phase changes.

Considering the results, under these milling conditions, the most important variable in producing structure amorphization is the zirconium content of the binary alloy.

Acknowledgements

References

Aguilar, C., Guzmán, D., Castro, F., Martínez, V., de Las Cuevas, F., Lascano, S., & Muthiah, T. (2014). Fabrication of nanocrystalline alloys Cu–Cr–Mo super satured solid solution by mechanical alloying. *Materials Chemistry and Physics*, *146(3)*, 493-502.
DOI: 10.1016/j.matchemphys.2014.03.060

Arias, D., & Abriata, J. P. (1990). Cu-Zr (copper-zirconium). *Journal of Phase Equilibria*, *11(5)*, 452-459.
DOI: 10.1007/BF02898260

Benjamin, J. S., & Volin, T. E. (1974). The mechanism of mechanical alloying. *Metallurgical Transactions*, *5(8)*, 1929-1934. DOI:10.1007/BF02644161

Benjamin, J. S. (1970). Dispersion strengthened superalloys by mechanical alloying. *Metallurgical transactions*, *1(10)*, 2943-2951. DOI:10.1007/BF03037835

Bera, S., Chowdhury, S. G., Lojkowsky, W., & Manna, I. (2012). Synthesis of CuCr and CuCrAg alloys with extended solid solubility with nano-Al 2 O 3 dispersion by mechanical alloying and consolidation by high pressure sintering. *Materials Science and Engineering*: A, *558*, 298-308. DOI: 10.1016/j.msea.2012.08.004

Betancourt-Cantera, J. A., Sánchez-De Jesús, F., Torres-Villaseñor, G., Bolarín-Miró, A. M., & Cortes-Escobedo, C. A. (2012). Extended solid solubility of a Co–Cr system by mechanical alloying. *Journal of Alloys and Compounds*, 529, 58-62. DOI: 10.1016/j.jallcom.2012.03.082

Brandstetter, S., Derlet, P. M., Van Petegem, S., & Van Swygenhoven, H. (2008). Williamson–Hall anisotropy in nanocrystalline metals: X-ray diffraction experiments and atomistic simulations. Acta Materialia, *56(2)*, 165-176. DOI: 10.1016/j.actamat.2007.09.007

Brunelli, K., Dabala, M., Frattini, R., Sandona, G., & Calliari, I. (2001). Electrochemical behaviour of Cu–Zr and Cu–Ti glassy alloys. *Journal of alloys and compounds*, *317*, 595-602. DOI: 10.1016/S0925-8388 (00)01394-3

Calka, A., & Radlinski, A. P. (1991). Universal high performance ball-milling device and its application for mechanical alloying. *Materials Science and Engineering*: A, *134*, 1350-1353. DOI:10.1016/0921-5093(91)90989-Z

Contini, A., Delogu, F., Garroni, S., Mulas, G., & Enzo, S. (2014). Kinetics behaviour of metastable equiatomic Cu–Fe solid solution as function of the number of collisions induced by mechanical alloying. *Journal of Alloys and Compounds*, *615*, S551-S554. DOI: 10.1016/j.jallcom.2013.11.232

Chen, T. R., & Lee, P. Y. (1993). Formation of amorphous Cu–Zr alloy powder by mechanical alloying. *Journal of Marine Science and Technology-Taiwan*, *1(1)*, 59-64. Retrieved from: http://jmst.ntou.edu.tw/marine/1/59-64.pdf

Davis, R. M., McDermott, B., & Koch, C. C. (1988). Mechanical alloying of brittle materials. *Metallurgical Transactions A*, *19(12)*, 2867-2874. Doi:10.1007/BF02647712

Delogu, F., & Cocco, G. (2006). Crystallite size refinement in elemental species under mechanical processing conditions. *Materials Science and Engineering*: A, *422(1)*, 198-204. DOI: 10.1016/j.msea.2006.02.032

Du, J., Wen, B., Melnik, R., & Kawazoe, Y. (2014). Phase stability, elastic and electronic properties of Cu–Zr binary system intermetallic compounds: A first-principles study. *Journal of Alloys and Compounds*, *588*, 96-102. DOI: 10.1016/j.jallcom.2013.11.018

Fecht, H. J., Hellstern, E., Fu, Z., & Johnson, W. L. (1990). Nanocrystalline metals prepared by high-energy ball milling. *Metallurgical Transactions A, 21(9)*, 2333-2337. DOI:10.1007/BF02646980

Hamzaoui, R., & Elkedim, O. (2013). Magnetic properties of nanocrystalline Fe–10% Ni alloy obtained by planetary ball mills. *Journal of Alloys and Compounds, 573*, 157-162. DOI: 10.1016/j.jallcom.2013.03.183

He, X. C., Wang, H., Liu, H. S., & Jin, Z. P. (2006). Thermodynamic description of the Cu–Ag–Zr system. *Calphad, 30(4)*, 367-374. DOI: 10.1016/j.calphad.2006.09.001

Kubalova, L. M., & Fadeeva, V. I. (2014). The effect of deformation treatment on the decomposition of supersaturated Ni (Nb, B) and Ni (Mo, B) solid solutions synthesized by mechanical alloying. *Journal of Alloys and Compounds*, *586*, S61-S64. DOI: 10.1016/j.jallcom.2012.10.115

Kumar, A., Jayasankar, K., Debata, M., & Mandal, A. (2015). Mechanical alloying and properties of immiscible Cu-20 wt.% Mo alloy. *Journal of Alloys and Compounds, 647*, 1040-1047. DOI: 10.1016/j.jallcom.2015.06.129

Kursun, C., & Gogebakan, M. (2015). Characterization of nanostructured Mg–Cu–Ni powders prepared by mechanical alloying. *Journal of Alloys and Compounds, 619*, 138-144. DOI: 10.1016/j.jallcom.2014.08.126

Loginov, P. A., Levashov, E. A., Kurbatkina, V. V., Zaitsev, A. A., & Sidorenko, D. A. (2015). Evolution of the microstructure of Cu–Fe–Co–Ni powder mixtures upon mechanical alloying. *Powder Technology, 276*, 166-174. DOI: 10.1016/j.powtec.2015.02.020

Loureiro, J. M., Costa, B. F., Malaman, B., Le Caër, G., Das, S., & Amaral, V. S. (2014). Formation stages of bcc (Fe 44 Co 44) Sn 12 extended solid solution by mechanical alloying. *Journal of Alloys and Compounds, 615*, S559-S563. DOI: 10.1016/j.jallcom.2013.12.071

Lu, L. (1998). Man On Lai, Mechanical Alloying.

Maurice, D., & Courtney, T. H. (1992). Modeling of the mechanical alloying process. JOM, 44(8), 10-14. DOI: 10.1007/BF03222293

Nazari, A., & Zakeri, M. (2013). Modeling the mean grain size of synthesized nanopowders produced by mechanical alloying. *Ceramics International, 39(2)*, 1587-1596. DOI: 10.1016/j.ceramint.2012.07.111

Okamoto, H. (2008). Cu-Zr (copper-zirconium). *Journal of phase equilibria and diffusion, 29(2),* 204-204. DOI: 10.1007/s11669-008-9267-2

Fang, Q., & Kang, Z. (2015). An investigation on morphology and structure of Cu–Cr alloy powders prepared by mechanical milling and alloying. Powder Technology, 270, 104-111. DOI: 10.1016/j.powtec.2014.10.010

Ristić, R., Cooper, J. R., Zadro, K., Pajić, D., Ivkov, J., & Babić, E. (2015). Ideal solution behaviour of glassy Cu–Ti, Zr, Hf alloys and properties of amorphous copper. *Journal of Alloys and Compounds, 621*, 136-145. DOI: 10.1016/j.jallcom.2014.09.167

Rojas, P. A., Peñaloza, A., Wörner, C. H., Fernández, R., & Zúñiga, A. (2006). Supersaturated Cu–Li solid solutions produced by mechanical alloying. *Journal of alloys and compounds*, *425(1)*, 334-338. DOI: 10.1016/j.jallcom.2006.01.032

Schwarz, R. B., & Koch, C. C. (1986). Formation of amorphous alloys by the mechanical alloying of crystalline powders of pure metals and powders of intermetallics. *Applied Physics Letters, 49(3)*, 146-148.

Suryanarayana, C. (1995). Nanocrystalline materials. *International Materials Reviews, 40(2),* 41-64. DOI: 10.1179/imr.1995.40.2.41

Suryanarayana, C. (2004). *Mechanical alloying and milling*. CRC Press.

Suryanarayana, C., & Inoue, A. (2010). *Bulk metallic glasses*. CRC Press.

Suryanarayana, C. (2001). Mechanical alloying and milling. *Progress in materials science, 46(1),* 1-184. DOI: 10.1016/S0079-6425 (99)00010-9

Ungár, T. (2004). Microstructural parameters from X-ray diffraction peak broadening. *Scripta Materialia*, *51(8)*, 777-781. DOI: 10.1016/j.scriptamat.2004.05.007

Vishlaghi, M. B., & Ataie, A. (2014). Investigation on solid solubility and physical properties of Cu–Fe/CNT nano-composite prepared via mechanical alloying route. *Powder Technology*, *268*, 102-109. DOI: 10.1016/j.powtec.2014.08.010

Wu, Z., & Bei, H. (2015). Microstructures and mechanical properties of compositionally complex CO-free Fe-NiMnCr 18 FCC solid solution alloy. *Materials Science and Engineering: A, 640*, 217-224. DOI: 10.1016/j.msea.2015.05.097

Xu, D., Lohwongwatana, B., Duan, G., Johnson, W. L., & Garland, C. (2004). Bulk metallic glass formation in binary Cu-rich alloy series–Cu 100– x Zr x (x= 34, 36, 38.2, 40 at.%) and mechanical properties of bulk Cu 64 Zr 36 glass. *Acta Materialia, 52(9),* 2621-2624. DOI: 10.1016/j.actamat.2004.02.009

Zhang, A., Chen, D., & Chen, Z. (2009). Bulk metallic glass-forming region of Cu–Zr binary and Cu–Zr based multicomponent alloy systems. *Journal of Alloys and Compounds, 477(1)*, 432-435. DOI: 10.1016/j.jallcom.2008.10.022

Xu D., B. Lohwongwatana, G. Duan, W. Johnson, C. Garland. (2004). Bulk metallic glass formation in binary Cu-rich alloy series – Cu100–xZrx (x=34, 36, 38.2, 40 at.%) and mechanical proper-ties of bulk Cu64Zr36 glass. Acta Mater 52, 2621-2624. DOI: 10.1016/j.actamat.2004.02.009

Zhang A., D. Chen, Z. Chen. (2009). Bulk metallic glass-forming region of Cu–Zr binary and Cu–Zr based multicomponent alloy systems. J. Alloy Compd. 477, 432-435. DOI: 10.1016/j.jallcom.2008.10.022